Nano Energy 65 (2019) 103998

Contents lists available at ScienceDirect

Nano Energy

journal homepage: www.elsevier.com/locate/nanoen

Full paper

An ultra-thin colored textile with simultaneous solar and passive heating abilities

Hao Luo[a], Qiang Li[a,*], Kaikai Du[a], Ziquan Xu[a], Huanzheng Zhu[a], Dongli Liu[b,c], Lu Cai[a], Pintu Ghosh[a], Min Qiu[b,c]

[a] State Key Laboratory of Modern Optical Instrumentation, College of Optical Science and Engineering, Zhejiang University, Hangzhou, 310027, China
[b] Key Laboratory of 3D Micro/Nano Fabrication and Characterization of Zhejiang Province, School of Engineering, Westlake University, 18 Shilongshan Road, Hangzhou, 310024, China
[c] Institute of Advanced Technology, Westlake Institute for Advanced Study, 18 Shilongshan Road, Hangzhou, 310024, China

ARTICLE INFO

Keywords:
Radiative textile
Energy-saving thermal management
Nanophotonics

ABSTRACT

Personal thermal management, especially heating up the space around human body, consumes substantial global resources. While traditional methods (such as room heaters) for personal heating are mostly energy-wasting and eco-unfriendly, ultra-thin textile with localized heating ability has recently gained significant attention. To date, passive radiative heating textiles are designed exclusively for indoor scenario and the coloration remains challenging. Herein, the authors report a colored nanophotonic structure textile (~16 μm thickness) with localized heating ability for both indoor and outdoor environments: (a) solar heating by selectively absorbing sunlight and converting it into heat (maximum absorbance ~ 50%) and (b) passive heating by suppressing radiative heat loss with a low-emissivity outer surface (infrared emissivity ~ 10%). This textile enables a 3.8 °C temperature enhancement of the artificial skin in indoor environment and a 6.3 °C temperature enhancement under sunlight compared with 2-mm-thick black sweatshirt, as well as excellent aesthetics, wearability and manufacturability. This colored textile with simultaneous solar and passive heating abilities is effective for energy-saving personal thermal management, and paves an innovative way to the sustainable development.

1. Introduction

Towards preventing cold-related injuries and illnesses, heating up the space around human body for thermal comfort consumes substantial resources and contributes to environmental issues such as air pollution and global warming [1–4]. Most part of energy consumed for indoor temperature regulation by traditional room heating devices is wasted in maintaining a comfortable temperature range in large empty spaces [5–7]. Studies show that if the indoor heating set-point can be decreased by 4 °C, 35% of the total consumed energy can be saved [8]. Meanwhile, traditional room heating devices can hardly be utilized for personal heating in outdoor environments, where cold-related health threats are more likely to happen because of uncontrollable temperature fluctuations [9–12]. Outdoor personal heating, therefore, is of paramount importance just like indoor heating as inevitable outdoor activities are important parts of our day-to-day life.

Wearing protective clothes is vital and cost-effective for personal heating in both indoor and outdoor environments. However, as the air gap between clothes and skin is narrow, clothes can be easily heated to a temperature a little higher than the ambient temperature. This temperature difference leads to radiative heat loss from the cloth to the ambience, and the radiative heat loss rate can be calculated following the formula (The human body covered with the cloth is assumed to be enclosed by the environment and the surface area of the cloth is assumed to be much smaller than that of the enclosure [13].)

$$q_{rad} \approx \sigma \varepsilon_{cloth} (T_{cloth}^4 - T_{amb}^4) \quad (1)$$

where ε_{cloth} is the surface emissivity of the cloth, σ is the Stefan-Boltzmann constant, T_{cloth} and T_{amb} are the temperatures of the cloth and the ambience, respectively. Commercially available insulating textile like cotton has high surface emissivity ($\varepsilon_{cloth} \sim 0.89$) [5] in the mid-infrared (MIR) thermal radiation wavelength regime. Although it can be made thick for better insulation against convection and conduction, huge radiative loss is inevitable. Aiming for cost-effective personal thermal management, thinner radiative textiles with better control of the surface emissivity have recently been demonstrated. (such as radiative

Abbreviations: nPE, nanoporous polyethylene; PDA, polydopamine; WVTR, water vapor transmission rate

* Corresponding author.
E-mail address: qiangli@zju.edu.cn (Q. Li).

https://doi.org/10.1016/j.nanoen.2019.103998
Received 31 May 2019; Received in revised form 6 August 2019; Accepted 7 August 2019
Available online 09 August 2019
2211-2855/

cooling [6,14–18], radiative heating [5–7] and adaptive radiative textile [20], details provided in Table S1). However, conventional radiative textiles like Mylar blanket, which is made up of thin plastic (usually polyethylene terephthalate) coated with dense metallic coatings (Al or Ag), can hardly be used for daily wear due to its poor breathability and wettability [5]. To address these problems, Ag nanowire-coated textile [7] and metallized radiative heating textile [5,6] with superior heating ability have been experimentally demonstrated.

While these passive-heating textiles are exclusively focused on the indoor heating, the research on ultra-thin textiles manifesting optimal heating ability in the outdoor environment is still lacking; moreover, the coloration of radiative heating textiles, which is significant for aesthetic or functional reasons, is also challenging. Compared to the indoor environment, outdoor radiative loss is more severe as a large part of thermal radiation from clothes can reach the cold outer space (T_{amb} = 3K) through the atmospheric window [14,19–25], bringing extra difficulties on efficient outdoor personal heating. Nevertheless, outdoor solar irradiation has the potential to act as a renewable external source for vast energy-harvesting applications including personal heating [26–30].

In this article, to realize optimal radiative heating ability without sacrificing wearability and aesthetic need, an ultra-thin (~16 μm in thickness) colored nanophotonic structure textile with simultaneous outdoor solar heating (solar energy absorption ~ 50%) and passive radiative heating (infrared emissivity ~ 10%) abilities is reported. The textile is fabricated by depositing ultra-thin gold (Au) and germanium (Ge) optical coatings onto a polydopamine (PDA)-coated nanoporous polyethylene (nPE) textile. This textile with simultaneous solar and passive heating abilities presents several advantageous traits. (1) Excellent heating ability: indoor and outdoor (under sunlight irradiation) thermal measurements reveal that it helps increase the artificial skin temperature by 3.8 °C and 6.3 °C compared to the black sweatshirt, respectively. (2) Ultra-thin thickness: its thickness is 16 μm while its heating performance is comparable to 5.2-mm-thick black sweatshirt. (3) Excellent aesthetics and wearability: vivid colors (orange, magenta, purple and blue) can be enabled by varying the deposition time of Ge; its breathability, mechanical strength and wettability are comparable to conventional textiles like the black sweatshirt and Mylar blanket. (4) Easy manufacturability: the nPE substrate is the widely available separator used in lithium-ion battery industry and with low price; optical coatings involve only film deposition, which is free from pollution of liquid waste, as distinct from conventional dyeing [31] or electroplating [32] processes. We believe this ultra-thin colored textile with simultaneous solar and passive heating abilities can not only help in reducing power consumption globally but also contribute to the environmental protection.

2. Results and discussion

The underlying physical mechanisms of colored heating textiles with simultaneous solar and passive heating abilities, as well as conventional textiles and passive radiative heating textiles, are illustrated in Fig. 1a, where q_{net} denotes the net heat flux from the textile into the skin. Conventional heating textiles like black sweatshirts achieve localized heating because of their broadband absorption in visible wavelength range; however, they also feature inevitable high radiative loss owing to their high surface emissivity. For better heating performance, the conventional textiles have to be thick to lower down the outer surface temperature. Typical passive radiative heating textiles like Mylar blanket reflects infrared light as well as sunlight, thus hardly absorbing sunlight in the outdoor environment. In this work, by simultaneously engineering the absorption and reflection in the spectral regions of the solar radiation (ultra-violet (UV), visible (VIS) and near infrared (NIR)) and the human body radiation (mid-infrared (MIR)), an ultrathin heating textile combining solar heating (broadband high solar absorption) and passive heating (broadband low MIR radiation) can be designed.

The colored nanophotonic structure textile with simultaneous solar and passive heating abilities is demonstrated with nanoporous textile coated by ultra-thin spectrally-selective optical coatings (SEM image shown in Fig. S2, Supplementary Material). The nanoporous (pore size < 200 nm in diameter and ~16 μm in thickness) PE textile with good breathability is adopted as the substrate. The ultra-thin coating consists of a layer of lossy Ge (< 20 nm in thickness) and an optically thick Au layer (~ 80 nm in thickness). The lossy Ge layer and the Au layer support strong interference effects in the UV-VIS-NIR region [33–35], enabling angle-independent spectrally-selective broadband solar absorption [33]. As a result, the ultra-thin optical coating presents three major functionalities: (1) solar heating ability due to the broadband solar absorption in the lossy Ge layer, (2) passive heating owing to the low MIR radiation because of the highly reflective Au coating and (3) coloration (orange, magenta, purple and blue) without iridescence [34] due to the selective visible absorption.

As a proof of concept, we record the optical (Fig. 1b) and thermal (Fig. 1c) images of a toy sheep partially covered by the colored nanophotonic structure textile with simultaneous solar and passive heating abilities. As shown in the thermal image, the uncovered parts of the toy sheep as well as the surrounding leaves and grass are in warmer colors because they behave as blackbody emitters in MIR range. The middle part of the toy sheep covered with the colored textile and facing the clear sky is in colder colors, indicating that both emitted and reflected energy from this part is extra low. The back and abdomen parts of the toy sheep are in warmer colors due to the diffused reflection of the radiation emitted by the surroundings (further verified when the textiles are placed facing the sky (Fig. S3, Supplementary Material) and the covered toy sheep in indoor environment (Fig. S4, Supplementary Material)).

2.1. Heat transfer model analysis

In order to evaluate the impact of textiles' optical properties on personal heating in both indoor and outdoor environments, a steady-state one-dimensional heat transfer model considering heat loss (radiative loss, convective/conductive heat loss) as well as metabolic heat generation [5,16] is adopted (details provided in Supplementary Notes, Supplementary Material). For the indoor environment, the net heat flux (q_{net}) can be defined by

$$q_{net} = q_{sur} - q_{conv} - q_{cond} - q_{rad} \quad (2)$$

where q_{sur} is the heat gain rate due to the absorbed thermal radiation from the surroundings (assumed as blackbody emitters), q_{conv} , q_{cond} and q_{rad} are heat loss rates through convection, conduction and radiation, respectively. Assuming that the room temperature is 21 °C (arbitrarily chosen low temperature) and the skin temperature is maintained at 34 °C, the equilibrium heat generation rate from skin is dependent on the inner surface emissivity (ε_{in}) and outer surface emissivity (ε_{out}) of the covered textiles (Fig. 1d, details about contributions of different forms of heat loss are provided in Fig. S5a, Supplementary Material). As the outer surface emissivity increases, the heating ability of the textile drops off; higher heat generation rate is thus required to maintain the skin temperature. With the same thickness (16 μm, which is the thickness of the nPE textile used in this work), the net heat flux (metabolic heat generation rate) from the skin covered by textiles with low outer surface emissivity (ε_{out} = 0.1) can be reduced to 56.1% of that covered by conventional textiles (ε_{out} = 0.89, the emissivity of cotton [5]). In other words, the cotton should be as thick as 5.2 mm to gain the same heating ability as that of the 16-μm-thick textile with an outer surface emissivity of 0.1 (calculation results and experimental demonstration provided in Fig. S6, Supplementary Material).

The outdoor solar heating ability(under sunlight) is analyzed by taking the absorbed solar irradiation as well as the absorbed atmospheric thermal radiation into consideration (details provided in

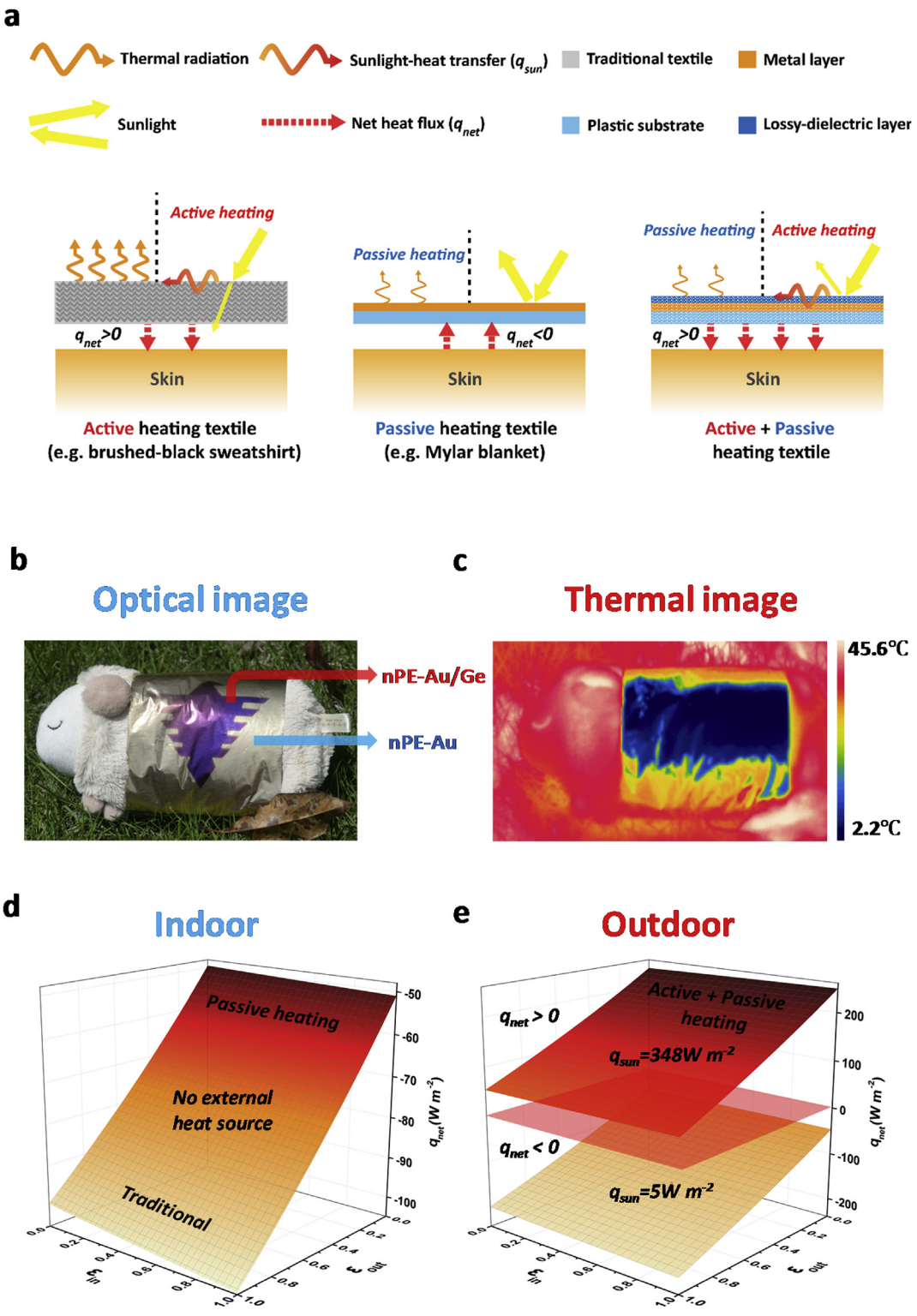

Fig. 1. Colored textile absorbs sunlight with suppressed thermal emission for localized personal heating. (a) Schematics depicting the heating mechanism of different textiles (conventional heating, passive radiative heating and colored textile with simultaneous solar and passive heating abilities). q_{net} denotes the net heat flux from the textile into the skin. (b), (c) Optical and thermal images of a toy sheep partly wearing a colored textile with simultaneous solar and passive heating abilities. (d) Calculated net heat flux q_{net} as functions of the textile's inner surface emissivity (ε_{in}) and outer surface emissivity (ε_{out}) in the indoor environment. The room temperature is set as 21 °C and the constant skin temperature is 34 °C. (e) Calculated net heat flux q_{net} as functions of ε_{in} and ε_{out} in the outdoor environment. Two textiles with different solar absorption abilities are considered: colored textile with simultaneous solar and passive heating abilities (q_{sun} = 348 W m^{-2}) and Mylar blanket (q_{sun} = 5 W m^{-2}). The upper area (q_{net} > 0) and lower area (q_{net} < 0) indicate net heat flux towards and outwards from the skin, respectively. The analysis highlights the two key ingredients for achieving excellent heating performance: maximization of the solar absorption for solar heating and minimization of outer surface emissivity for passive heating.

Supplementary Notes, Supplementary Material). The net heat flux from the textile towards the human body can be defined as

$$q_{net} = q_{sun} + q_{atm} - q_{conv} - q_{cond} - q_{rad} \quad (3)$$

where q_{sun} is the heat gain rate due to solar absorption and is given by

$$q_{sun} = \cos(\phi) \int d\lambda a_{VIS-NIR}(\lambda, \phi) I_{AM1.5}(\lambda) \quad (4)$$

where ϕ is the angle between normal direction of the textile and the sun, $a_{VIS-NIR}$ indicates the spectral angular absorptivity and $I_{AM1.5}(\lambda)$ is the solar radiation on earth during daytime, q_{atm} is the heat gain rate due to the absorption of atmospheric radiation (details provided in Supplementary Text). At constant environmental temperature (21 °C) and skin temperature (34 °C), the net heating flux q_{net} as functions of inner surface emissivity ε_{in} and outer surface emissivity ε_{out} for different absorbed solar power can be calculated (Fig. 1e, details about contributions of different forms of heat loss are provided in Fig. S5b, Supplementary Material). For simplicity, two absorbed solar power values are considered here (assuming $\phi = 47°$): $q_{sun} = 348\ \mathrm{W\,m^{-2}}$ for the colored textile with simultaneous solar and passive heating abilities (the case for nPE-Au/Ge (15 nm)) and $q_{sun} = 5\ \mathrm{W\,m^{-2}}$ for a single Al coating with negligible solar absorption (the case for Mylar blanket). Due to their low solar absorbance, passive heating textiles like Mylar blanket can hardly trap solar energy for localized personal heating, metabolic heat generation is thus needed ($q_{net} < 0$) because of the inevitable convection heat loss. For conventional textile like cotton ($\varepsilon_{out} = 0.89$), the radiative heat loss through atmospheric window results in high demand for metabolic heat generation when the textile is with low solar absorbance. In contrast, the textile which efficiently convert sunlight into heat and simultaneously suppresses thermal radiation has its apparent advantages on personal thermal management.

2.2. Optical properties

The colored nanophotonic structure textile with simultaneous solar and passive heating abilities is demonstrated by constructing thin optical coatings (Au and Ge) onto nPE textile and the color is tuned by varying the deposition time of Ge layer. The deposition rate of Ge is $1\ \mathrm{Å\,s^{-1}}$ and the deposition time varies from 80 s to 200 s. To make the textile suitable for daily wearing, the polydopamine (PDA) coating is performed on the nPE textile to enhance wettability [36–38] before the deposition of ultra-thin optical coatings (see Material and Methods for details).

The thermal radiation properties of different textiles (Fig. 2a) are measured by a Fourier transform infrared spectrometer. For the fabricated colored textiles with simultaneous solar and passive heating abilities, the measured MIR emissivities of both inner surfaces ($\varepsilon_{in} \sim 0.34$) and outer surfaces ($\varepsilon_{out} \sim 0.10$) are far smaller than the conventional textiles like black sweatshirts (with both ε_{in} and $\varepsilon_{out} \sim 0.80$). The outer surface emissivity of the colored textiles with simultaneous solar and passive heating abilities is also comparable to that of the Mylar blanket (emission from the Al coating side, $\varepsilon_{out} \sim 0.10$). Although the Ge thickness varies for obtaining different textile colors, the outer surface emissivity of the colored textiles with simultaneous solar and passive heating abilities is not influenced owing to their ultrathin property (a maximum thickness of ~20 nm for Ge) (Fig. S7a, Supplementary Material). Incidentally, the slight increase in the inner surface emissivity of the textiles with simultaneous solar and passive heating abilities can be attributed to the PDA coatings (Fig. S7b, Supplementary Material).

Besides low emissivity for passive heating, high solar absorption is another key to the efficient solar heating. The ultrathin dielectric coating (Ge) introduce spectrally-selective broadband solar absorption, enabling solar heating as well as coloration. The cut-off wavelength for solar absorption redshifts as the deposition time of Ge coating increases and different colors can be obtained (8 nm: orange, 12 nm: magenta, 16 nm: purple, 20 nm: blue, corresponding to the chromaticity provided in Fig. S8, Supplementary Material). As a result, the corresponding solar absorption increases with the Ge deposition time (8 nm: 26.2%, 12 nm: 37.2%, 16 nm: 50.2% and 20 nm: 50.8%). Therefore, the solar heating capability of the colored textile (see Fig. S9, Supplementary Material, for calculated solar absorbance for Ge coatings with different thicknesses) can be even higher than the black sweatshirt which has a broadband solar absorption of ~38.3% (with a solar transmittance ~25%, see Fig. S10a, Supplementary Material, for details).

2.3. Heating performance

The indoor measurements for passive heating ability are performed inside an acrylic chamber (Fig. 3a), in which a constant temperature (21 ± 0.5 °C) is maintained. A black insulating tape (artificial skin) on a silicone rubber heater is used to simulate human skin as their emissivities ($\varepsilon \sim 1$ for black tape and $\varepsilon \sim 0.95$ for the human skin, see Fig. S11b, Supplementary Material for the measured emissivity of the insulating tape) are comparable. The silicone rubber heater beneath the black insulating tape, which is connected to a DC supply, generates heat to simulate metabolic heat generation. By periodically turning the heater on and off, the real-time temperature of the artificial skin covered with different textiles is recorded (Fig. 3b and c). The artificial skin covered by colored textile with simultaneous solar and passive heating abilities shows temperature increases of 9.4 °C and 3.8 °C compared to the bare skin and that covered by sweatshirt, respectively. The fast temperature rise rate of the artificial skins covered by textiles such as the resulting textile and Mylar blanket also indicates that low outer surface emissivity is the key for efficient indoor passive personal heating. Furthermore, to get the warmth-to-weight ratio comparison between thick sweatshirt and resulting textile, we measured the input power for heater to maintain constant skin temperature (33.5 °C) when covered with different textiles and the results agrees well with theoretical analysis (Fig. S6b, Supplementary Material).

The outdoor heating performance of the textiles is measured in a clear bright sunny day (30th September, 2018) on a roof top inside Yuquan campus, Zhejiang University (Fig. 3d, see Material and methods for details). The experimental setup is placed under sunlight and exposed to wind. Fig. 3e plots the measured temperature of artificial skins covered with different textiles including the blue textile with simultaneous solar and passive heating abilities (with Ge thickness of 20 nm) with recording time is from 11:00 to 14:00 (local time). The blue textile with simultaneous solar and passive heating abilities has the maximum solar absorbance (50%) among all tested textiles and enables average temperature of the artificial skin to be 6.3 °C higher than that covered by black sweatshirt, manifesting excellent solar heating performance. Besides, the solar heating ability of the sweatshirt is overestimated in this experiment as the transmitted light through the sweatshirt is absorbed by the black tape (Fig. S10a, Supplementary Material), which is more absorptive than the true skin. Compared to bare gold coating, the ultra-thin Ge coating enables the average temperature of the artificial skin to be 13.7 °C higher. For textiles with simultaneous solar and passive heating abilities with different colors, the solar absorbance is different, resulting in different heating abilities (Fig. 3f). Compared with the textile with a bare gold coating, the average temperature of the artificial skin is enhanced by 6.2 °C, 9.8 °C, 12.2 °C and 13.7 °C for the textile with simultaneous solar and passive heating abilities with different Ge thickness (8 nm, 12 nm, 16 nm and 20 nm, respectively).

2.4. Wearability tests

As the textiles are for daily wearing, their wearability performance is crucial for practical applications. The wearability is usually characterized in several aspects: breathability (WVTR (water vapor transmission rate)), air permeability, mechanical strength and wettability. The breathability of the colored textile with simultaneous solar and passive heating abilities is tested with the one coated with thickest

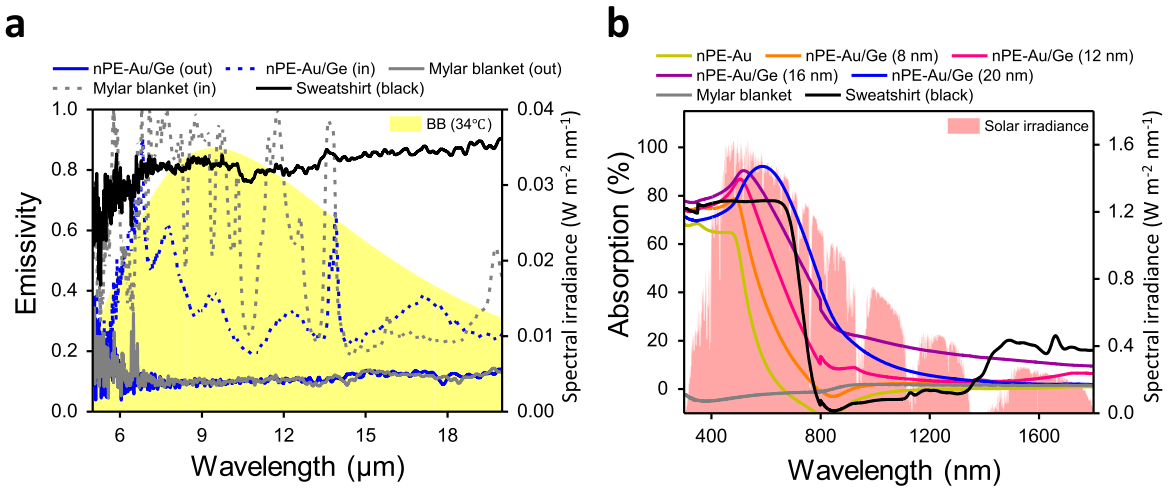

Fig. 2. Optical property of the textiles. (a) Measured emissivity of different textiles. The blue solid and dashed lines are for outer and inner surface emissivities of the colored textile with simultaneous solar and passive heating abilities, respectively. The gray solid and dashed lines are for outer and inner surface emissivities of the Mylar blanket, respectively. The black line is for the black sweatshirt. The light yellow area denotes the spectral irradiance of the blackbody at 34 °C. (b) Measured absorptivity of different textiles from visible to near infrared wavelengths. The pale green line is for the heating textile with a single gold film. For the textile with simultaneous solar and passive heating abilities with different Ge deposition time (8 nm, 12 nm, 16 nm and 20 nm), the colors of the absorption curves represent the corresponding display color (orange, magenta, purple and blue, respectively). The dark gray and black lines are for the Mylar blanket and the black sweatshirt, respectively. The pale red area denotes the solar spectral irradiance. (For interpretation of the references to color in this figure legend, the reader is referred to the Web version of this article.)

optical coatings (~80 nm Au and ~20 nm Ge). The nanopores (with sizes below 200 nm) in the textile allow water vapor from perspiration to be transmitted from the skin outwards (Fig. 4a and b). While the coatings have slight impact on the WVTR (Fig. S12, Supplementary Material), the textile exhibits similar breathability to the normal textile like sweatshirt, both of which are much higher than that of the Mylar blanket (Fig. 4b). This textile is also windproof because of its extra low air permeability (Fig. 4c). Its air permeability is comparable with that of the Mylar blanket and can prevents wind form blowing in and carrying heat away [15]. The resulting textile exhibits a breaking strength of ~30 N, higher than that of the Mylar blanket (Fig. 4d), rendering itself strong enough to withstand high tensile force. For the wettability measurement, the water contact angle of textile with simultaneous solar and passive heating abilities without polydopamine (PDA) deposition is 128°, which is hydrophobic (Fig. 4e). By extending the PDA deposition time (30 min and 45 min), the textile with simultaneous solar and passive heating abilities turns hydrophilic as the water contact angle is decreased to 77° and 55°, respectively.

Furthermore, the heating ability of the 16-μm-thick textile with simultaneous solar and passive heating abilities is comparable to the 5.2-mm-thick sweatshirt (Fig. S2, Supplementary Material) while being much thinner (Fig. 4f), thus providing a solution for reducing thickness and weight of winter outwears. The weight of the textile with simultaneous solar and passive heating abilities is 12.6 g m^{-2}, which is much lighter than the Mylar blanket (17.4 g m^{-2}) and conventional textiles like black sweatshirt (269.4 g m^{-2}). We further demonstrated that the optical coatings on nPE remain even after peeled by an adhesive tape, showing robust adhesion of the coatings to nPE (Supplementary Movie S1). The nPE based colored textile can be knitted with conventional textiles such as cotton for better wear comfort as long as its surface facing the environment (Fig. S13). The optical coatings can also be applied for typical commercial textiles like polyester fibers and expanded PTFE (which is widely used for waterproof textiles) for coloration and low surface emissivity (Fig. S14, Supplementary Material).

Supplementary video related to this article can be found at https://doi.org/10.1016/j.nanoen.2019.103998.

We note that the aluminum, which is an abundant and cheap material, can replace the notable metal when worked with ultra-thin amorphous silicon (in place of Ge) for colored textiles with simultaneous solar and passive heating abilities (Fig. S15, Supplementary Material). The nPE textile is commercially available ($ 2.6 m^{-2}) and is widely used in lithium-ion battery industry as separator. Since the pore sizes of PE separator adopted are mostly under 200 nm, the resulting textile allows less amount of metals for low emissivity (~50 nm in thickness, Fig. S16, Supplementary Material) compared to the previously demonstrated passive heating textile (~150 nm in thickness) [6].

3. Conclusion

In summary, we demonstrate an ultra-thin colored textile with simultaneous solar and passive heating abilities. This colored heating textile is made of a PDA-coated nanoporous textile coated with a reflective metal layer and an ultra-thin lossy dielectric layer. Strong interference induced by the optical coatings leads to broadband selective solar absorption, which enables the textile to present solar heating ability as well as vivid colors. Meanwhile, the textile maintains low MIR emissivity (< 0.1) for passive heating. The artificial skin covered with this textile attains temperatures of 3.8 °C/6.4 °C higher as compared to that covered with a 2-mm thick black sweatshirt in indoor/outdoor environments. We note that, the near infrared absorptivity of the textile is around 34% which can potentially be improved by designing optical coatings with more complicated structures [29,39]. Furthermore, this textile is ultra-thin (thickness ~ 16 μm), light-weight (12.6 g m^{-2}), and has comparable wearability to conventional textiles. The PDA coating method not only enhances the wearability but also has potential for endowing antibacterial performance due to copper ions chelated with the coatings [38]. We believe that this colored textile with simultaneous solar and passive heating abilities can not only help reducing global energy waste on temperature regulation but also contribute to solving the health issues especially for outdoor activities in the frigid environment without sacrificing aesthetics.

4. Material and Methods

Textile Fabrication: The nPE separator was bought from SK Innovation. The Au and Ge were deposited onto the nPE film in the chamber of a high vacuum magnetic sputtering system (MSP-6600,

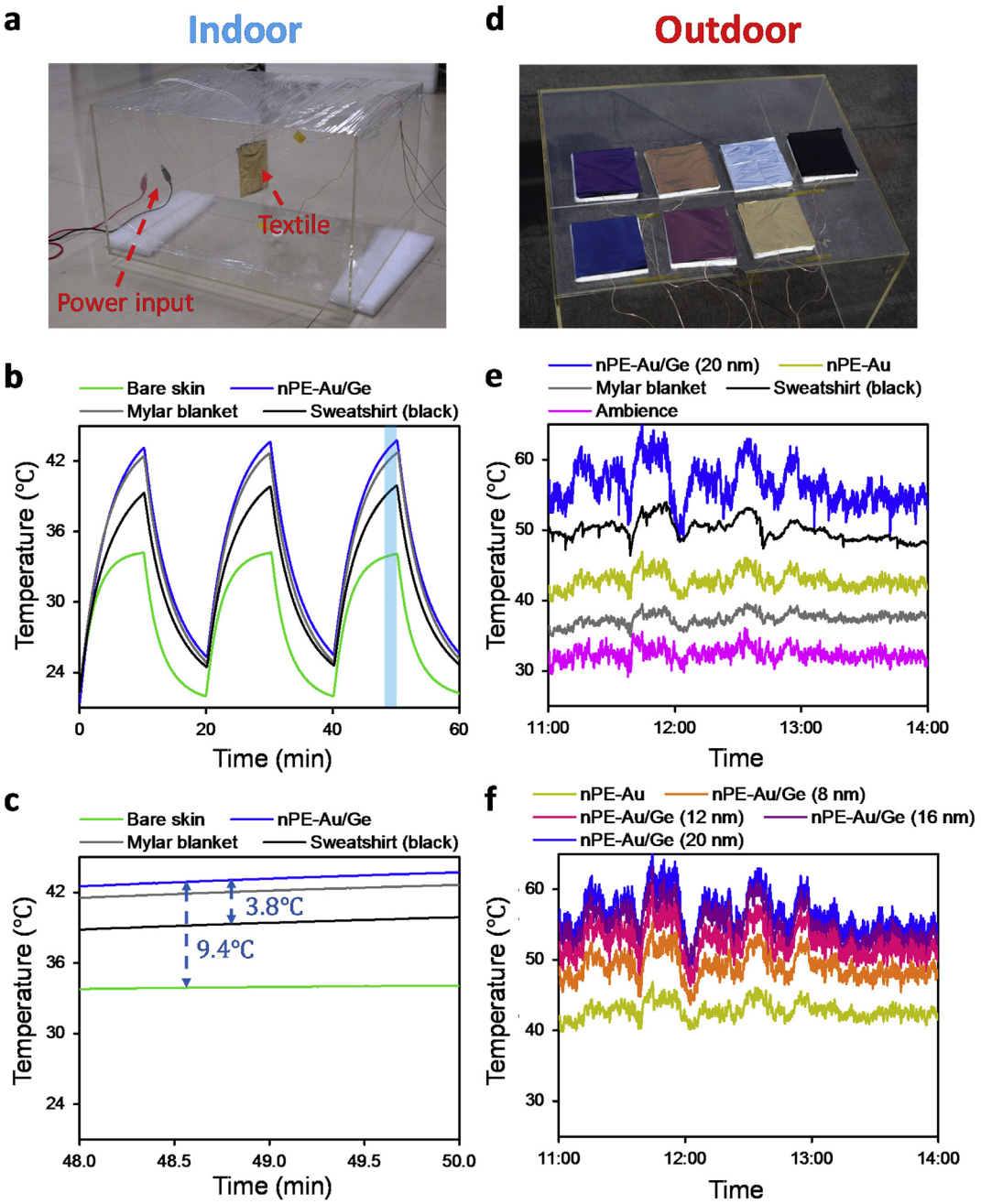

Fig. 3. Localized heating ability of the colored textiles. (a) Experimental setup for indoor thermal measurement. (b) Measured real-time temperatures of the artificial skins covered with different textiles in indoor environment with environmental temperature controlled at 21 ± 0.5 °C. The power input (heater) is periodically turned on and off. (c) Close-up view of b showing the temperature differences during the time interval from 48 min to 50 min. (d) Experimental setup for outdoor thermal measurement. Top row (from left to right: nPE-Au/Ge (16 nm), nPE-Au/Ge (8 nm), Mylar blanket and black sweatshirt). Down row (from left to right: nPE-Au/Ge (20 nm), nPE-Au/Ge (12 nm) and nPE-Au). (e), (f) Real-time temperatures of artificial skins covered with (e) different textiles and (f) textile with simultaneous solar and passive heating abilities with different colors in the outdoor environment under wind convection. (For interpretation of the references to color in this figure legend, the reader is referred to the Web version of this article.)

Beijing Jingshengweina Technology Co., Ltd). The deposition rates for Au and Ge were both 1 Å s^{-1}. Before deposition, the nPE was treated with polydopamine (PDA) for better wettability. The solution for PDA coating was prepared by dissolving dopamine hydrochloride (2 mg mL^{-1}) in a Tris buffer solution (pH = 8.5, 50 mM) with $CuSO_4$ (1.25 mg mL^{-1}) and H_2O_2 (2 μL mL^{-1}). The method for PDA coating has the advantage of reduced construction time and improved uniformity [36]. The deposition rate for PDA coating was 43 nm h^{-1}. After deposition, the nPE was rinsed in deionized (DI) water.

Thermal measurement: All thermal measurements were performed with a thermocouple (Omega, SA-1K) and a Keithley 2700 multimeter was used to acquire the real-time temperature. The tested black sweatshirt was Gildan 88000 made of 50% cotton and 50% polyster. Indoor part: A silicone rubber electric heater connected to a DC supply provided heat generation with a rate of 130 W m^{-2}. An aluminum foil was firstly pasted on the heater's surface to make the temperature uniform. A black insulating tape, whose emissivity was very close to the real skin (Fig. S11, Supplementary Material), was then pasted on the aluminum foil to form the artificial skin. The temperature is measured with the artificial skin covered with different textiles.

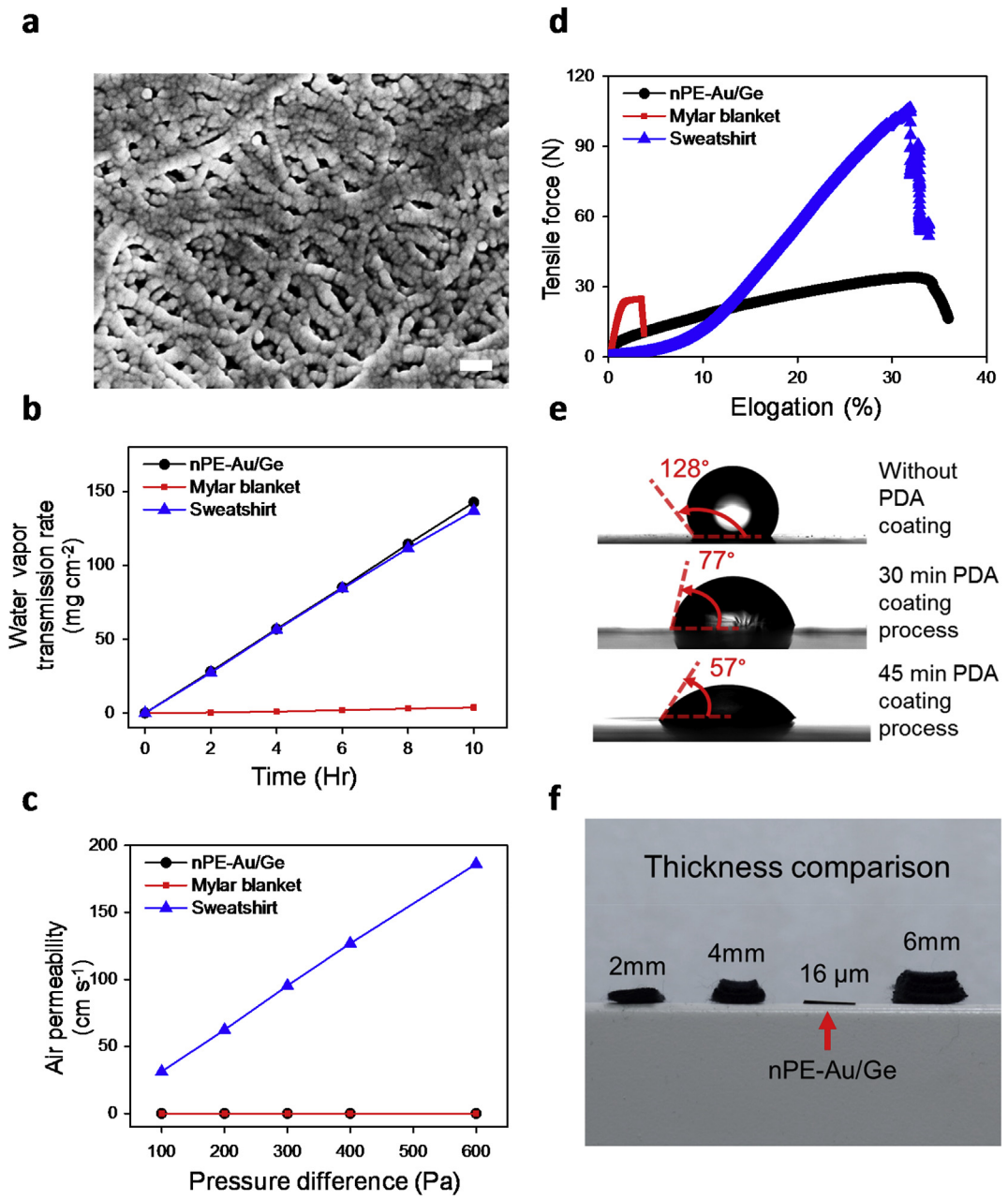

Fig. 4. Wearability of the colored textiles. (a) An SEM image of the outer surface of the colored textile with simultaneous solar and passive heating abilities. The scale bar is 200 nm. Measured (b) water vapor transmission rate, (c) air permeability and (d) tensile strength of different textiles (textile with simultaneous solar and passive heating abilities, Mylar blanket and sweatshirt). (e) Water contact angle measurement for the inner surface of textile with simultaneous solar and passive heating abilities without and with PDA coating process. (f) Thickness comparison of the resulting textile (nPE-Au/Ge) with black sweatshirts with different thicknesses (2 mm, 4 mm and 6 mm). The heating ability of textile with simultaneous solar and passive heating abilities is comparable to 5.2 mm thick black sweatshirt.

Outdoor part: The artificial skin was made of a piece of glass (9 mm × 9 mm in size, 1 mm in thickness) wrapped with the black insulating tape which was highly absorptive in all wavelength of interests (Fig. S11, Supplementary Material). A 6-mm-thick aerogel was used to hold the artificial skin which acted as a heat insulator. All artificial skins covered with different textiles were exposed to sunlight (facing the sky) and the temperatures were recorded in local time. The thermal image of Fig. 1c was taken by a thermal camera (FLIR, ThermaCAM S65).

Optical characterization: MIR part: Emissivities of different textiles were measured with a Fourier transform infrared spectrometer (Bruker, Vertex 70) equipped with a room-temperature doped triglycine sulfate (DTGS) detector. The black soot deposited onto a gold-coated silicon wafer using a burning candle was used as a reference. Different samples were fixed on the same heater controlled by a temperature controller. The temperature was set as 60 °C during characterization. UV-VIS-NIR part: Transmission and reflection spectra were measured using a universal measurement spectrophotometer (Agilent, Cary7000) equipped with an integrate sphere. The incident angle of light source was about 8°. For the measurement of diffuse reflectance, a silver film deposited on a BK7 glass was used as a reference.

Water vapor transmission rate test: The test was performed using ASTM E96 with modification. Petri dishes filled with 10 ml distilled water were sealed by the textile samples using rubber bands. These sealed dishes were then put into an environmental chamber whose temperature was kept at 35 °C and relative humidity inside at 30%. The dishes were weighed periodically with an electronic balance (OHAUS, AR1502CN). The water vapor transmission rates were calculated from

the mass loss, which was equal to the mass of evaporated water.

Air permeability test: The air permeability test was performed with a digital fabric air permeability meter (YG461E, Quanzhou Meibang Instrument Co., Ltd) based on ASTM D737 with modification. The exposed area of the textile was 20 cm^2. By setting different values of pressure difference between upper and lower surfaces of the textile, the air flow rates were measured.

Mechanical test: The tensile strength test was measured by a dynamic mechanical analysis machine (Q800). The textile samples were cut into rectangular shape (2 cm × 5 cm). The gauge distance was 3 cm long and the displacement rate was 10 mm min^{-1}.

Water contact angle measurement: The static water contact angles were measured by a DropMeter A-200 contact angle system (MAIST Vision Inspection & Measurement Co. Ltd., China) in the ambient environment to evaluate the wettability of the textile.

Author contributions

Q.L. conceived the idea and supervised the project together with M.Q. H. L performed the calculations and experiments. P.G. performed part of the calculation. L.C. performed part of the fabrication. K.D., Z.X., H.Z. and D.L. performed part of the characterization. H.L., Q.L. and M.Q. wrote the manuscript. All authors discussed the results and contributed to the final version of the manuscript.

Funding

This work is supported by National Key Research and Development Program of China (2017YFA0205700 and 2017YFE0100200) and National Natural Science Foundation of China (Grant Nos. 61425023, 61575177 and 61775194).

Conflicts of interest

The authors declare no competing financial interest.

Acknowledgements

We gratefully acknowledge discussions with Mingbang Wu (Department of Polymer Science and Engineering, Zhejiang University), Yue Zhang (College of Chemical and Biological Engineering, Zhejiang University), Mingkai Cao (College of Optical Science and Engineering, Zhejiang University), and Biao Feng, Shuaiqi Tian(School of Energy Engineering, Zhejiang University) on polydopamine coating process, tensile strength measurement, chromaticity diagram measurement, and breathability measurements, respectively.

Appendix A. Supplementary data

Supplementary data to this article can be found online at https://doi.org/10.1016/j.nanoen.2019.103998.

References

[1] US Energy Information Administration, Annual Energy Outlook 2018 with Projections to 2050, US Energy Information Administration, Office of Energy Analysis, (2018) https://www.eia.gov/outlooks/aeo/pdf/AEO2018.pdf , Accessed date: 31 May 2019.
[2] D&R International, Ltd, Buildings Energy Data Book, US Department of Energy, Energy Efficiency and Renewable Energy Department, 2011, http://large.stanford.edu/courses/2015/ph240/davidson1/docs/2011_BEDB.pdf , Accessed date: 31 May 2019.
[3] UK National Institute for Health and Care Excellence, Costing Statement: Excess Winter Deaths and Illness Implementing the NICE Guidance on Excess Winter Deaths and Illnesses Associated with Cold Homes (NG6), UK National Institute for Health and Care Excellence, 2015, https://www.nice.org.uk/guidance/ng6/resources/costing-statement-pdf-6811741 , Accessed date: 31 May 2019.
[4] PRC National Development and Reform Commission, Planning for Heating and Cleaning in Winter in Northern China (2017-2021), PRC National Development and Reform Commission, 2017, http://www.gov.cn/xinwen/2017-12/20/5248855/files/7ed7d7cda8984ae39a4e9620a4660c7f.pdf , Accessed date: 31 May 2019.
[5] L. Cai, A.Y. Song, P. Wu, P.C. Hsu, Y. Peng, J. Chen, C. Liu, P.B. Catrysse, Y. Liu, A. Yang, C. Zhou, Warming up human body by nanoporous metallized polyethylene textile, Nat. Commun. 8 (2017) 496 https://doi.org/10.1038/s41467-017-00614-4.
[6] P.C. Hsu, C. Liu, A.Y. Song, Z. Zhang, Y. Peng, J. Xie, K. Liu, C.L. Wu, P.B. Catrysse, L. Cai, S. Zhai, A dual-mode textile for human body radiative heating and cooling, Sci. Adv. 3 (2017) e1700895https://doi.org/10.1126/sciadv.1700895.
[7] P.C. Hsu, X. Liu, C. Liu, X. Xie, H.R. Lee, A.J. Welch, T. Zhao, Y. Cui, Personal thermal management by metallic nanowire-coated textile, Nano Lett. 15 (2015) 365–371 https://doi.org/10.1021/nl5036572.
[8] T. Hoyt, K.H. Lee, H. Zhang, E. Arens, T. Webster, Presented at International Conference on Environmental Ergonomics, Boston, 2009.
[9] T.M. Mäkinen, J. Harris, Health problems in cold work, Ind. Health 47 (2009) 207–220 https://doi.org/10.2486/indhealth.47.207.
[10] W. Kirch, B. Menne, R. Bertollini, Extreme Weather Events and Public Health Responses, Springer, 2005.
[11] F. Brocherie, O. Girard, G.P. Millet, Emerging environmental and weather challenges in outdoor sports, Climate 3 (2015) 492–521 https://doi.org/10.3390/cli3030492.
[12] H. Brändström, G. Johansson, G.G. Giesbrecht, K.A. Ängquist, M.F. Haney, Accidental cold-related injury leading to hospitalization in northern Sweden: an eight-year retrospective analysis, Scand. J. Trauma. Resus. 22 (2014) 6 https://doi.org/10.1186/1757-7241-22-6.
[13] Michael Modest, Radiative Heat Transfer, Academic Press, 2003, p. 173.
[14] L. Cai, A.Y. Song, W. Li, P.C. Hsu, D. Lin, P.B. Catrysse, Y. Liu, Y. Peng, J. Chen, H. Wang, J. Xu, Spectrally selective nanocomposite textile for outdoor personal cooling, Adv. Mater. (2018) 1802152 https://doi.org/10.1002/adma.201802152.
[15] P.C. Hsu, A.Y. Song, P.B. Catrysse, C. Liu, Y. Peng, J. Xie, S. Fan, Y. Cui, Radiative human body cooling by nanoporous polyethylene textile, Science 353 (2016) 1019–1023 https://doi.org/10.1126/science.aaf5471.
[16] J.K. Tong, X. Huang, S.V. Boriskina, J. Loomis, Y. Xu, G. Chen, Infrared-transparent visible-opaque fabrics for wearable personal thermal management, ACS Photonics 2 (2015) 769–778 https://doi.org/10.1021/acsphotonics.5b00140.
[17] Y. Peng, J. Chen, A.Y. Song, P.B. Catrysse, P.C. Hsu, L. Cai, B. Liu, Y. Zhu, G. Zhou, D.S. Wu, H.R. Lee, Nanoporous polyethylene microfibres for large-scale radiative cooling fabric, Nat. Sustain. 1 (2018) 105 https://doi.org/10.1038/s41893-018-0023-2.
[18] G.J. Lee, Y.J. Kim, H.M. Kim, Y.J. Yoo, Y.M. Song, Colored, daytime radiative coolers with thin-film resonators for aesthetic purposes, Adv. Opt. Mater. 6 (2018) 1800707 https://doi.org/10.1002/adom.201800707.
[19] X.A. Zhang, S. Yu, B. Xu, M. Li, Z. Peng, Y. Wang, S. Deng, X. Wu, Z. Wu, M. Ouyang, Y. Wang, Dynamic gating of infrared radiation in a textile, Science 363 (2019) 619–623 http://doi.org/10.1126/science.aau1217.
[20] A.P. Raman, M.A. Anoma, L. Zhu, E. Rephaeli, S. Fan, Passive radiative cooling below ambient air temperature under direct sunlight, Nature 515 (2014) 540 https://doi.org/10.1038/nature13883.
[21] Y. Zhai, Y. Ma, S.N. David, D. Zhao, R. Lou, G. Tan, R. Yang, X. Yin, Scalable-manufactured randomized glass-polymer hybrid metamaterial for daytime radiative cooling, Science 355 (2017) 1062–1066 https://doi.org/10.1126/science.aai7899.
[22] J. Mandal, Y. Fu, A.C. Overvig, M. Jia, K. Sun, N.N. Shi, H. Zhou, X. Xiao, N. Yu, Y. Yang, Hierarchically porous polymer coatings for highly efficient passive daytime radiative cooling, Science 362 (2018) 315–319 https://doi.org/10.1126/science.aat9513.
[23] Z. Chen, L. Zhu, A. Raman, S. Fan, Radiative cooling to deep sub-freezing temperatures through a 24-h day–night cycle, Nat. Commun. 7 (2016) 13729 https://doi.org/10.1038/ncomms13729.
[24] L. Zhu, A. Raman, S. Fan, Color-preserving daytime radiative cooling, Appl. Phys. Lett. 22 (2013) 223902 https://doi.org/10.1063/1.4835995.
[25] M.M. Hossain, M. Gu, Radiative cooling: principles, progress, and potentials, Adv. Sci. 7 (2016) 1500360 https://doi.org/10.1002/advs.201500360.
[26] Wei Wang, Yurui Qu, Kaikai Du, Songang Bai, Jingyi Tian, Meiyan Pan, Hui Ye, Min Qiu, Qiang Li, Broadband optical absorption based on single-sized metal-dielectric-metal plasmonic nanostructures with high-ε" metals, Appl. Phys. Lett. 10 (2017) 101101 http://doi.org/10.1063/1.4977860.
[27] Li Qiang, Jun Lu, Prince Gupta, Min Qiu, Engineering optical absorption in graphene and other 2D materials: advances and applications, Adv. Optical Mater. 7 (2019) 1900595 https://doi.org/10.1002/adom.201900595.
[28] J. Mandal, D. Wang, A.C. Overvig, N.N. Shi, D. Paley, A. Zangiabadi, Q. Cheng, K. Barmak, N. Yu, Y. Yang, Scalable, "Dip-and-Dry" fabrication of a wide-angle plasmonic selective absorber for high-efficiency solar-thermal energy conversion, Adv. Mater. 29 (2017) 1702156 https://doi.org/10.1002/adma.201702156.
[29] W. Li, Y. Shi, Z. Chen, S. Fan, Photonic thermal management of coloured objects, Nat. Commun. 9 (2018) 4240 https://doi.org/10.1038/s41467-018-06535-0.
[30] Z. Chen, L. Zhu, W. Li, S. Fan, Simultaneously and synergistically harvest energy from the sun and outer space, Joule 3 (2018) 101–110 https://doi.org/10.1016/j.joule.2018.10.009.
[31] H. Zangeneh, A.A.L. Zinatizadeh, M. Habibi, M. Akia, M.H. Isa, Photocatalytic oxidation of organic dyes and pollutants in wastewater using different modified titanium dioxides: a comparative review, J. Ind. Eng. Chem. 26 (2015) 1–36 https://doi.org/10.1016/j.jiec.2014.10.043.
[32] B. Navinšek, P. Panjan, I. Milošev, PVD coatings as an environmentally clean alternative to electroplating and electroless processes, Surf. Coat. Tech. 116 (1999) 476–487 https://doi.org/10.1016/S0257-8972(99)00145-0.
[33] M.A. Kats, R. Blanchard, P. Genevet, F. Capasso, Nanometre optical coatings based on strong interference effects in highly absorbing media, Nat. Mater. 12 (2013) 20

https://doi.org/10.1038/nmat3443.
[34] M.A. Kats, F. Capasso, Optical absorbers based on strong interference in ultra-thin films, Laser Photonics Rev. 10 (2016) 735–749 https://doi.org/10.1002/lpor.201600098.
[35] M.A. Kats, F. Capasso, Ultra-thin optical interference coatings on rough and flexible substrates, Appl. Phys. Lett. 105 (2014) 131108 https://doi.org/10.1063/1.4896527.
[36] C. Zhang, Y. Ou, W.X. Lei, L.S. Wan, J. Ji, Z.K. Xu, CuSO4/H2O2-induced rapid deposition of polydopamine coatings with high uniformity and enhanced stability, Angew. Chem. Int. Ed. 55 (2016) 3054–3057 https://doi.org/10.1002/anie.201510724.
[37] M.H. Ryou, Y.M. Lee, J.K. Park, J.W. Choi, Mussel-inspired polydopamine-treated polyethylene separators for high-power Li-ion batteries, Adv. Mater. 23 (2011) 3066–3070 https://doi.org/10.1002/adma.201100303.
[38] H. Lee, S.M. Dellatore, W.M. Miller, P.B. Messersmith, Mussel-inspired surface chemistry for multifunctional coatings, Science 318 (2017) 426–430 https://doi.org/10.1126/science.1147241.
[39] F. Chen, S.W. Wang, X. Liu, R. Ji, L. Yu, X. Chen, W. Lu, High performance colored selective absorbers for architecturally integrated solar applications, J. Mater. Chem. A 3 (2015) 7353–7360 https://doi.org/10.1039/C5TA00694E.

Hao Luo received the B.Sc. degree from Zhejiang University, Hangzhou, China, in 2016. He also obtained honors degrees of Chu Kechen Honors College in Zhejiang University. His research interest focuses on cost-effective personal thermal management and nanophotonic devices incorporating phase-change chalcogenides.

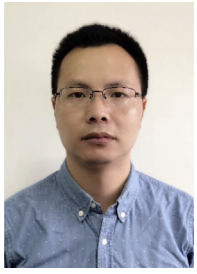

Prof. Qiang Li received the B.Sc. degree and M. Eng from the Harbin Institute of Technology, Harbin, China, in 2005 and 2007, respectively. He obtained the Ph.D. degree in Microelectronics and Applied Physics from the Royal Institute of Technology (KTH), Stockholm, Sweden, in 2011. In 2011 he joined College of Optical Science and Engineering, Zhejiang University, as an assistant professor. He became an associate professor in 2013 and a full professor in 2017. His research interest focuses on energy-efficient silicon-/metal-based optoelectronic materials, devices and their applications in optical communications and energy utilization.

Dr. Kaikai Du received the B.Sc. degree from the Zhejiang University, Hangzhou, China. He obtained his Ph.D. degree from Zhejiang University, in 2018. His research interest focus on tunable thermal emitters consist of phase-change materials such as GST and VO_2.

Ziquan Xu is a Ph.D. candidate in the Laboratory of Integrated Photonics and Nanophotonics, Zhejiang University. He obtained his B.Sc degree from Nankai University, Tianjing, China. His current project is adaptive thermal management and spatial modulation of thermal emission with direct laser writing system and phase change materials.

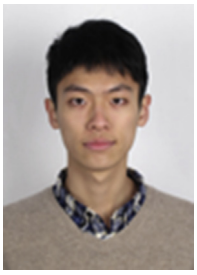

Huanzheng Zhu received the B.Sc. degree from Zhejiang University, Hangzhou, China, in 2016. He also obtained honors degrees of Chu Kechen Honors College in Zhejiang University. His research interest focuses on multiband optical camouflage and thermal management for objects with high temperature.

Dr. Dongli Liu received his Ph.D. degree in Refrigeration and Cryogenic Engineering from Zhejiang University, China in 2017. Currently, he is a Research Fellow at Westlake University, China. His research interests focus on advanced micro and nano refrigeration methods.

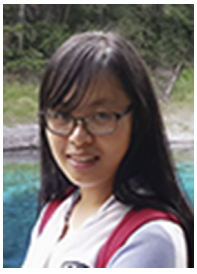

Lu Cai is a Ph.D. candidate in the Laboratory of Integrated Photonics and Nanophotonics, Zhejiang University. She received the B.Sc. degree from Shandong University. She is now a visiting student in Prof. David Wright's group in the University of Exeter. Her research interest focuses on engineering thermal emission with polar materials and phase change materials.

Prof. Pintu Ghosh received Ph.D. degree in Physics from Indian Institute of Technology Bombay, India in 2016. He worked as a postdoctoral research fellow at College of Optical Science and Engineering, Zhejiang University, and later became an assistant professor at the same college in 2019. His research interests include nanofabrication, nonlinear optics, and thermal emission from nanostructures.

Prof. Min Qiu received the Ph.D. degree in Physics from Zhejiang University, China in 1999. He became an assistant professor and a full professor at the Royal Institute of Technology (KTH), Sweden, in 2001 and 2009, respectively. Since 2010, he worked as a professor at Zhejiang University. He was the Director of State Key Laboratory of Modern Optical Instrumentation, Zhejiang University. In 2018 he joined Westlake University as a Chair Professor of Photonics and Vice President for Research. His research interests include nanofabrication technology, nanophotonics, and green photonics.